MODELLISTICA E CALCOLO SCIENTIFICO

MODELING AND SCIENTIFIC COMPUTING

MOX–Report No. 08/2007

Fluid-structure interaction problems in free surface flows: application to boat dynamics

Luca Formaggia, Edie Miglio,
Andrea Mola, Nicola Parolini

MOX, Dipartimento di Matematica "F. Brioschi"
Politecnico di Milano, Via Bonardi 29 - 20133 Milano (Italy)

mox@mate.polimi.it http://mox.polimi.it

Fluid-structure interaction problems in free surface flows: application to boat dynamics*

L. Formaggia(1), E. Miglio(1), A. Mola(1), N. Parolini(2)

April 27, 2007

(1) MOX– Modellistica e Calcolo Scientifico
Dipartimento di Matematica "F. Brioschi"
Politecnico di Milano
via Bonardi 9, 20133 Milano, Italy
luca.formaggia@polimi.it, edie.miglio@polimi.it, andrea.mola@polimi.it

(2) CMCS - Institut d'Analyse et Calcul Scientifique
Ecole Polytechnique Fédérale de Lausanne
Station 8, CH-1015, Lausanne, Switzerland
nicola.parolini@epfl.ch

Keywords: Computational Fluid Dynamics, Fluid structure interaction, Dynamics of rowing

AMS Subject Classification: 76T10, 74F10, 65M60

Abstract

In this paper we present some recent studies on fluid-structure interaction problems in the presence of free surface flow. We consider the dynamics of boats simulated as rigid bodies. Several hydrodynamic models are presented, ranging from full Reynolds Averaged Navier-Stokes equations down to reduced models based on potential flow theory.

1 Introduction

The use of computational fluid dynamics (CFD) in boat design is traditionally based on potential flow theory, even if in the last years the use of Reynolds Averaged Navier-Stokes (RANS) codes has become increasingly more common. The role of CFD is of particular importance whenever performance optimisation is critical, such as in competition boat, where even a small advantage may be

*This work has been supported by a joint project with Filippi Lido s.r.l.

crucial. An overview on the numerical techniques for ship hydrodynamics may be found in [4, 3] and, more specifically, their relevance for high performance sailing boat in [14].

In this field, most of the numerical investigations aim to assess the boat characteristics at a given fixed configuration. Furthermore, they usually compute a steady state solution, even if sometimes this is reached through pseudo time stepping. Yet, simulating the full dynamics of a boat may be of great importance [1, 15]. We mention two cases: high performance sailing boats and rowing sculls. In the former, the accurate simulation of the dynamics may allow for a better trimming of the boat [1, 16], better evaluating wave resistance [13] and in perspective the assessment of its performance during manoeuvring. For a competition rowing scull, accounting for the dynamics effects is even more important. Indeed, because of the periodic action at the oars and the movement of the oarsmen on the boat the motions of the scull is very complex and characterised by horizontal accelerations/decelerations, sinking and dipping. These secondary movements generate waves which dissipate part of rowers energy, which could be better spent to move the boat forward.

In this paper, we will give an account of our research in this class of problems. We give first a general framework to describe the dynamics of a boat under the action of the hydrodynamic and other external forces, describing also its integration with RANS codes.

Transient computations using RANS models are computationally demanding, while in the design process there is the need of having tools for fast predictions to compare different design configurations. In the case of the rowing scull, the same tools may also be used to study the effect of different oarsmen layout or rowing style. We describe a reduced model for the scull dynamics, where the energy dissipation effects induced by the secondary motions are simulated by computing a suitable potential problem for wave radiation. Despite its simplicity, the approach has proved to be highly effective. Finally, we describe an intermediate model based on the solution of quasi-3D Navier-Stokes equations with free surface [10], where the presence of the boat is modelled through an inequality constraint. We show how the method is able to reproduce the general wave patterns of a moving scull.

2 The mathematical models

The simulation of the fluid dynamic field around a moving boat requires to account different aspects of the physics of the problem: the viscous effects (including those related to the turbulent nature of the flow) as well as the wave generation on the water free-surface. In this work, the structural deformations are not considered (since for the problems at hand their impact on the boat dynamics is negligible) and only the rigid body motion of the boat in the six degrees of freedom is modelled.

2.1 The Reynolds Averaged Navier-Stokes equations with free-surface

The hydrodynamic flow around the boat can be described by the so-called *Reynolds Averaged Navier-Stokes Equations*. In this approach, the turbulence effects are suitably modelled and enter the equations through an additional eddy viscosity term, avoiding the need of resolving the small scales (in time and space) which characterise turbulent flows. The presence of the *free surface* is accounted for by using a multiphase model, where the air flow in the vicinity of the boat is also computed.

Since we want to model the boat dynamics, we need to consider the problem defined on a computational domain $\Omega = \Omega(t)$ (and therefore a computational grid) that changes in time. In this situation, a convenient frame to cast the problem is the so-called Arbitrary Lagrangian Eulerian (ALE) approach [5, 6]. The equations to be solved are

$$\frac{\partial \rho}{\partial t}_{|\mathcal{A}} + (\boldsymbol{v} - \boldsymbol{v}_s) \cdot \boldsymbol{\nabla} \rho \quad = 0 \tag{1a}$$

$$\rho \frac{\partial \boldsymbol{v}}{\partial t}_{|\mathcal{A}} + \rho(\boldsymbol{v} - \boldsymbol{v}_s) \cdot \boldsymbol{\nabla} \boldsymbol{v} + \mathbf{div} \boldsymbol{T} \quad = \boldsymbol{f}_b \tag{1b}$$

$$\operatorname{div} \boldsymbol{v} \quad = 0. \tag{1c}$$

where ρ is the fluid density, p and $\boldsymbol{v}$ are the flow pressure and velocity, $\boldsymbol{T} = (\mu + \mu_t)(\nabla \boldsymbol{v} + \nabla^T \boldsymbol{v}) - p\boldsymbol{I}$ is the Cauchy stress tensor (with μ_t the turbulent viscosity) and $\boldsymbol{f}_b = \rho \boldsymbol{g}$ is the forcing term due to gravity. The term $\boldsymbol{v}_s$ is the domain velocity associated with the domain motion and the time derivatives are understood to be ALE time derivatives (we have used the special subscript $\mathcal{A}$ to indicate them). Density and viscosity are constant on the two subdomains containing air and water, respectively.

Boundary conditions are usually set by imposing a given velocity profile at the inflow, zero normal stresses at the outflow, symmetry condition on the far-field lateral boundaries and by forcing the velocity of the fluid to be equal to the velocity of the boat at the boat surface.

For the turbulence we adopt the $k - \varepsilon$ model [11] which requires the solution of two additional equations describing the evolution of the turbulent kinetic energy k and the turbulence dissipation rate ε.

The free-surface dynamics is tracked by using the *Volume of Fluid (VOF)* method, where the volume fraction c is used to identify the water ($c = 1$) from the air ($c = 0$) subdomain. A transport equation for c effectively replaces (1a) and reads

$$\frac{\partial c}{\partial t}_{|\mathcal{A}} + (\boldsymbol{v} - \boldsymbol{v}_s) \cdot \boldsymbol{\nabla} c = 0,$$

so that the variable density and viscosity can be defined based on the local value of c as follows:

$$\rho(\boldsymbol{x}) = c(\boldsymbol{x})\rho_w + (1 - c(\boldsymbol{x}))\rho_a, \quad \mu(\boldsymbol{x}) = c(\boldsymbol{x})\mu_w + (1 - c(\boldsymbol{x}))\mu_a,$$

where the suffixes w and a identify the water and the air, respectively. For details about the method the reader may refer to [7].

For the solution of system (1), a finite volume discretisation is adopted. It requires to solve for any cell V of the computational grid the following equations,

$$\frac{d}{dt}\int_V \rho(\boldsymbol{x})dV + \int_{\partial V} \rho(\boldsymbol{x})(\boldsymbol{v} - \boldsymbol{v}_s) \cdot d\boldsymbol{\gamma} = 0,$$

$$\frac{d}{dt}\int_V \rho(\boldsymbol{x})\boldsymbol{v}dV + \int_{\partial V} \rho(\boldsymbol{x})\boldsymbol{v}(\boldsymbol{v} - \boldsymbol{v}_s) \cdot d\boldsymbol{\gamma} = \int_{\partial V} \boldsymbol{T} \cdot d\boldsymbol{\gamma} + \int_V \boldsymbol{f}_b dV,$$

Similar finite volume discretisation can be obtained for the transport equations defining the turbulence model as well as for the volume fraction equation.

2.2 Modelling the boat rigid motion

A numerical method able to simulate the boat dynamics in calm water and waves requires the coupling between the fluid solver and a code for the structural dynamics.

Following the approach adopted in [1, 2], we consider two orthogonal Cartesian reference frames: an inertial reference system $(\boldsymbol{O}, X, Y, Z)$ which moves forward with the mean boat speed and a body-fixed reference system $(\boldsymbol{X}, x, y, z)$, whose origin is the boat centre of mass $\boldsymbol{X}$, which translates and rotates with the boat. The XY plane in the inertial reference system is parallel to the undisturbed water surface and the $Z - axis$ points upward. The body-fixed x-axis is directed from bow to stern and y is positive starboard.

The dynamics of the boat in the 6 degrees of freedom is described by the equations of linear and angular momentum, set in the inertial reference frame, and given by

$$M\ddot{\boldsymbol{X}} = \boldsymbol{F} \tag{3}$$

and

$$\mathcal{R}\mathcal{I}\mathcal{R}^{-1}\dot{\boldsymbol{\Omega}} + \boldsymbol{\Omega} \times \mathcal{R}\mathcal{I}\mathcal{R}^{-1}\boldsymbol{\Omega} = \boldsymbol{M}_G, \tag{4}$$

respectively. Here, M is the boat mass, $\ddot{\boldsymbol{X}}$ is the linear acceleration of the centre of mass, $\boldsymbol{F}$ are the force acting on the boat, $\dot{\boldsymbol{\Omega}}$ and $\boldsymbol{\Omega}$ are the angular acceleration and velocity, respectively. Finally, $\boldsymbol{M}_G$ is the moment with respect to G acting on the boat, $\mathcal{I}$ is the tensor of inertia of the boat about the body-fixed reference system axes and $\mathcal{R}$ is the transformation matrix between the body-fixed and the inertial reference system (see [1] for details).

The forces and moments acting on the boat can be expressed as

$$\begin{aligned}\boldsymbol{F} &= \boldsymbol{F}_{\text{Flow}} + M\boldsymbol{g} + \sum_{i=1}^{m} \boldsymbol{F}_{e_i} \\ \boldsymbol{M}_G &= \boldsymbol{M}_{\text{Flow}} + \sum_{i=1}^{m} (\boldsymbol{X}_{e_i} - \boldsymbol{X}) \times \boldsymbol{F}_{e_i},\end{aligned}$$

where $\boldsymbol{F}_{\text{Flow}}$ and $\boldsymbol{M}_{\text{Flow}}$ are the force and angular moment due to the interaction with the flow, $\boldsymbol{F}_{e_i}$ are external forcing terms (which may model, e.g., the wind force on sails or the inertial and traction forces due to the rowers action) while $\boldsymbol{X}_{e_i}$ are their application points.

To integrate in time the equations of motion, the second order ordinary differential equations (3-4) are formulated as systems of first order ODEs. If we consider, for example, the linear momentum equation (3), it can be rewritten as

$$M\dot{\boldsymbol{V}} = \boldsymbol{F}, \qquad \dot{\boldsymbol{X}} = \boldsymbol{V},$$

where $\boldsymbol{V}$ denotes the linear velocity of the centre of mass. This system is solved using an explicit 2-step Adam-Bashforth scheme for the velocity

$$\boldsymbol{V}^{n+1} = \boldsymbol{V}^n + \frac{\Delta t}{2M}(3\boldsymbol{F}^n - \boldsymbol{F}^{n-1}),$$

and a Crank-Nicholson scheme for the position of the centre of mass

$$\boldsymbol{X}^{n+1} = \boldsymbol{X}^n + \frac{\Delta t}{2}(\boldsymbol{V}^{n+1} + \boldsymbol{V}^n).$$

For a convergence analysis of the scheme (as well as for a detailed description of the integration scheme for the angular momentum equation), we refer to [8], where it is shown that second-order accuracy in time is obtained, and that the restriction on time step linked to numerical stability is less demanding than that required to capture the time evolution of this class of problems correctly.

In the fluid-structure interaction (FSI) problem the equilibrium configurations of the structure depends on the configurations of the fluid and vice-versa. In the coupling with the flow solver, the 6-DOF dynamical system receives at each time step the value of the forces and moments acting on the boat and returns values of new position as well as linear and angular velocity. In the flow solver, these data are used to update the computational grid (by a mesh motion strategy based on elastic analogy) and the flow equations (1) in ALE form are solved in the new domain.

2.3 The dynamics of a rowing boat

We now specialise the model for the case of a rowing boat. Due to the presence of rowers exerting on the hull intermittent traction and inertial forces, the main surging motion of a rowing boat is inevitably associated with some *secondary motions*. The latter cause a consistent additional drag component, mainly by wave radiation, and must therefore be considered to get accurate performance predictions.

Equations (3) and (4) in the case of a rowing boat driven by n rowers may be summarised as

$$M\ddot{\boldsymbol{X}} = \sum_{j=1}^{n} \boldsymbol{F}_{o_j} + \sum_{j=1}^{n} \boldsymbol{F}_{s_j} + \sum_{j=1}^{n} \boldsymbol{F}_{f_j} + M\boldsymbol{g} + \boldsymbol{F}_{\text{Flow}} \tag{5a}$$

$$\mathcal{R}\mathcal{I}\mathcal{R}^{-1}\dot{\boldsymbol{\Omega}} + \boldsymbol{\Omega} \times \mathcal{R}\mathcal{I}\mathcal{R}^{-1}\boldsymbol{\Omega} = \sum_{j=1}^{n} \left(\boldsymbol{X}_{o_j} - \boldsymbol{X}\right) \times \boldsymbol{F}_{o_j} + \sum_{j=1}^{n} \left(\boldsymbol{X}_{s_j} - \boldsymbol{X}\right) \times \boldsymbol{F}_{s_j} + \sum_{j=1}^{n} \left(\boldsymbol{X}_{f_j} - \boldsymbol{X}\right) \times \boldsymbol{F}_{f_j} + \boldsymbol{M}_{\text{Flow}}. \tag{5b}$$

where the angular momentum is computed around the hull barycentre. Here, $\boldsymbol{F}_{o_j}$, $\boldsymbol{F}_{s_j}$, $\boldsymbol{F}_{f_j}$ indicate the external forces exerted by each rower on oarlocks, seats and foot-boards, respectively. They can be obtained by the equations governing the dynamics of the rowers, as it follows.

We represent the mass distribution of an athlete of given characteristics (weight, height, sex) by subdividing the body into p parts of which we infer the mass m_{ij} from anatomical tables. We then write the momentum equations for the j-th rower as

$$\sum_{i=1}^{p} m_{ij} \left(\ddot{\boldsymbol{X}}_{ij} - \boldsymbol{g}\right) = \boldsymbol{F}_{h_j} + \boldsymbol{F}_{s_j} + \boldsymbol{F}_{f_j} \tag{6a}$$

$$\sum_{i=1}^{p} m_{ij} \left(\boldsymbol{X}_{ij} - \boldsymbol{X}_{f_j}\right) \times \left(\ddot{\boldsymbol{X}}_{ij} - \boldsymbol{g}\right) = \left(\boldsymbol{X}_{h_j} - \boldsymbol{X}_{f_j}\right) \times \boldsymbol{F}_{h_j} + \left(\boldsymbol{X}_{c_j} - \boldsymbol{X}_{f_j}\right) \times \boldsymbol{F}_{c_j}. \tag{6b}$$

Here, $\boldsymbol{F}_{h_j}$ is the force at the hand of the j-th athlete, while $\boldsymbol{X}_{h_j}$, $\boldsymbol{X}_{s_j}$ and $\boldsymbol{X}_{f_j}$ are the positions of the hands, seat and foot-board respectively. $\boldsymbol{X}_{ij}$ and $\ddot{\boldsymbol{X}}_{ij}$ indicate the position and acceleration of the barycentre of the i-th body part of the j-th rower, in the global reference frame. Finally, $\boldsymbol{X}_{f_j}$ is the position of the j-th foot-board. Writing equation (6b) we have neglected the contribution to the angular momentum due to each mass rotation around its own centre of mass.

Introducing into (5) the values for $\boldsymbol{F}_f$ and $\boldsymbol{F}_s$ obtained from (6), we get

$$M(\ddot{\boldsymbol{X}} - \boldsymbol{g}) = \sum_{j=1}^{n} \boldsymbol{F}_{o_j} + \sum_{j=1}^{n} \boldsymbol{F}_{h_j} - \sum_{j=1}^{n}\sum_{i=1}^{p} m_{ij}\left(\ddot{\boldsymbol{X}}_{ij} - \boldsymbol{g}\right) + \boldsymbol{F}_{\text{Flow}} \tag{7a}$$

$$\begin{aligned}\mathcal{R}\mathcal{I}\mathcal{R}^{-1}\dot{\boldsymbol{\Omega}} + \boldsymbol{\Omega} \times \mathcal{R}\mathcal{I}\mathcal{R}^{-1}\boldsymbol{\Omega} \;=\; & \sum_{j=1}^{n}\left(\boldsymbol{X}_{o_j} - \boldsymbol{X}\right) \times \boldsymbol{F}_{o_j} + \sum_{j=1}^{n}\left(\boldsymbol{X}_{h_j} - \boldsymbol{X}\right) \times \boldsymbol{F}_{h_j} \\ & - \sum_{j=1}^{n}\sum_{i=1}^{p} (\boldsymbol{X}_{ij} - \boldsymbol{X}) \times m_{ij}\left(\ddot{\boldsymbol{X}}_{ij} - \boldsymbol{g}\right) + \boldsymbol{M}_{\text{Flow}}. \end{aligned} \tag{7b}$$

We now assume that the motion of the boat lies in its symmetry plane (*i.e.*: only surge, heave and pitch motions are considered). This approximation is indeed valid for sculls, where each rower acts synchronously on both oars and we can reasonable assume that experienced rowers would minimise movements out of the symmetry plane. Indicating with lower case letters points in the relative reference frame we may write relations

$$\boldsymbol{X}_{ij} \;=\; \boldsymbol{X} + \mathcal{R}(\phi)\boldsymbol{x}_{ij} \tag{8a}$$

$$\ddot{\boldsymbol{X}}_{ij} \;=\; \ddot{\boldsymbol{X}} + \mathcal{R}(\phi)\ddot{\boldsymbol{x}}_{ij} + 2\dot{\phi}\mathcal{O}(\phi)\dot{\boldsymbol{x}}_{ij} + \ddot{\phi}\mathcal{O}(\phi)\boldsymbol{x}_{ij} - \dot{\phi}^2\mathcal{R}(\boldsymbol{\phi})\boldsymbol{x}_{ij} \tag{8b}$$

to link positions, velocities and accelerations in the two reference frames. Here, ϕ is the angle of rotation w.r.t. the y-axis while $\mathcal{R}$ and $\mathcal{O}$ are 2×2 rotation matrices, namely

$$\mathcal{R} = \begin{bmatrix} \cos\phi & -\sin\phi \\ \sin\phi & \cos\phi \end{bmatrix}, \qquad \mathcal{O} = \begin{bmatrix} -\sin\phi & -\cos\phi \\ \cos\phi & -\sin\phi \end{bmatrix}.$$

Substituting equations (8) in equations (7) we have finally that

$$\begin{aligned}(M + \sum_{i,j} m_{ij})\ddot{\boldsymbol{X}} + \mathcal{O}(\sum_{i,j} m_{ij}\boldsymbol{x}_{ij})\ddot{\phi} = -\mathcal{R}\sum_{j,j} m_{ij}\ddot{\boldsymbol{x}}_{ij} - 2\mathcal{O}(\sum_{i,j} m_{ij}\dot{\boldsymbol{x}}_{ij})\dot{\phi} \\ + \mathcal{R}(\sum_{i,j} m_{ij}\boldsymbol{x}_{ij})\dot{\phi}^2 + \sum_{j=1}^{n} \boldsymbol{F}_{o_j} + \sum_{j=1}^{n} \boldsymbol{F}_{h_j} + (M + \sum_{i,j} m_{ij})\boldsymbol{g} + \boldsymbol{F}_{\text{Flow}}\end{aligned} \tag{9a}$$

and

$$\begin{aligned}&\mathcal{R}(\sum_{i,j} m_{ij}\boldsymbol{x}_{ij}) \times \ddot{\boldsymbol{X}} + (I_{YY} + \sum_{i,j} m_{ij}|\boldsymbol{x}_{ij}|^2)\ddot{\phi} = \\ &- \mathcal{R}\sum_{i,j} m_{ij}\boldsymbol{x}_{ij} \times \mathcal{R}\ddot{\boldsymbol{x}}_{ij} - 2(\sum_{i,j} m_{ij}\mathcal{R}\boldsymbol{x}_{ij} \times \mathcal{O}\dot{\boldsymbol{x}}_{ij})\dot{\phi} + \sum_{i,j} m_{ij} \\ &+ \mathcal{R}\sum_{j=1}^{n} \boldsymbol{x}_{s_j} \times \boldsymbol{F}_{s_j} + \mathcal{R}\sum_{j=1}^{n} \boldsymbol{x}_{m_j} \times \boldsymbol{F}_{m_j}\mathcal{R}\sum_{i,j} m_{ij}\boldsymbol{x}_{ij} \times \boldsymbol{g} + \boldsymbol{M}_{\text{Flow}},\end{aligned} \tag{9b}$$

where in $\sum_{i,j}$ the indexes i and j run from 1 to p and 1 to n, respectively. Values for oarlock and hand forces (respectively $\boldsymbol{F_{o_j}}$ and $\boldsymbol{F_{h_j}}$) are provided by measurements on rowing machines, while the motion laws $\boldsymbol{x}_{ij}(t)$ for the rower body parts are measured by means of motion capture techniques [12].

Hence, equations (9) are a system of three nonlinear second order ordinary differential equations in the variables $(\boldsymbol{X}, \phi)$, that must be complemented by a suitable fluid dynamic model in order to compute $\boldsymbol{F}_{\text{Flow}}$ and M_{Flow} and close the problem. For instance, the RANS model just presented.

3 Reduced models for the FSI problem

An alternative to RANS simulations is to use simplified models to reduce the computational cost, while maintaining an acceptable accuracy.

3.1 Potential model for the calculation of the effects of secondary motions

In the first reduced model we present, forces and moments exerted on the hull by the surrounding fluid ($\boldsymbol{F}_{\text{Flow}}$ and M_{Flow} in equation (9)) are decomposed as follows,

$$\boldsymbol{F}_{\text{Flow}} = L_S \boldsymbol{e}_Z - D_S \boldsymbol{e}_X + \boldsymbol{F}_D, \qquad M_{\text{Flow}} = M_S + M_D. \tag{10}$$

Here L_S and M_S are the hydrostatic lift and moment which can be readily approximated from the instantaneous position of the hull. The total drag due to the primary surging motion D_S is computed by the formula

$$D_S = \frac{1}{2}\rho S_{\text{Ref}} C_{dX} (\dot{G}_X)^2,$$

where S_{Ref} is the wet surface, which again depends on the instantaneous position of the boat, and C_{dX} a drag coefficient, estimated for each boat by performing one (or more) Navier–Stokes simulations of the stationary motion.

The forces and moments due to the secondary motions of the boat, here indicated by $\boldsymbol{F}_D$ and M_D, respectively, are computed by solving in the computational domain Ω depicted in Fig. 1 the following Laplace problem [9] for the complex velocity potential ψ_α

$$\begin{aligned}
&\Delta\psi_\alpha = 0 && \text{on } \Omega, \\
&\frac{\partial\psi_\alpha}{\partial z} - \frac{\omega^2}{g}\psi_\alpha = 0 && \text{on } \Gamma_{fs}, \\
&\frac{\partial\psi_\alpha}{\partial n} - i\frac{\omega^2}{g}\psi_\alpha = 0 && \text{on } \Gamma_\infty, \qquad \alpha = 1,2,3. \\
&\frac{\partial\psi_\alpha}{\partial n} = 0 && \text{on } \Gamma_b, \\
&\frac{\partial\psi_\alpha}{\partial n} = N_\alpha && \text{on } \Gamma_c.
\end{aligned} \tag{11}$$

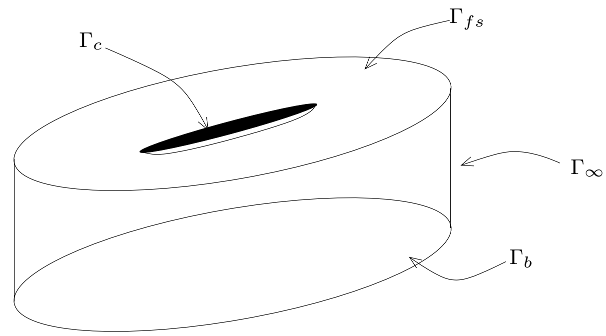

Figure 1: The computational domain for the potential problem (11)

From a physical point of view, it corresponds to solve three problems where a periodic motion of frequency $f = \omega/2\pi$ in the direction of the three degrees of freedom considered is imposed to the boat surface . The non-homogeneous Neumann conditions applied on the boat surface for each problem are therefore the components of the generalised normal vector $N = (n_x, n_z, zn_x - xn_z)$, being (n_x, n_y, n_z) the normal to the boat surface. A few simplifications were necessary to obtain the potential problem. In particular, a linearised form of the free surface interface conditions have been adopted and the equations are in fact solved in the reference configuration.

The forces due to secondary motions are finally computed by integrating the pressure on the boat surface. It turns out that these forces present a component proportional to the acceleration vector $(\ddot{\boldsymbol{X}}, \ddot{\phi})$, giving rise to an added mass matrix $\mathcal{M}$, and a component proportional to the velocity vector $(\dot{\boldsymbol{X}}, \dot{\phi})$, leading to a damping matrix $\mathcal{S}$. As for the angular velocity ω, we have taken the one which corresponds to the principal frequency of the motion of the rowers.

3.2 Models based on variational inequalities

Another possibility, alternative and of intermediate complexity with respect to RANS and the potential models, is to enforce the presence of a floating body in the context of the quasi-3D shallow water (3D-SW) formulation described in [10]. To illustrate the technique we consider a simplified system based on the hydrostatic approximation. This approximation reduces the vertical momentum equation to the static relation $\frac{\partial p}{\partial z} = -\rho g$. We also assume that the position of the free surface η can be described by a single-valued function of x and y, i.e $\eta = \eta(x, y, t)$ and that the water domain is given by $\Omega = \Omega_{2D} \times (-h, \eta)$, being h the quota of the water bottom (here taken constant) and Ω_{2D} a two-dimensional domain.

Under these hypotheses, the motion of the fluid can be described by the following system of equations

$$\begin{aligned}
&\frac{\partial \boldsymbol{u}}{\partial t} + (\boldsymbol{v}\cdot\boldsymbol{\nabla}_{xy})\,\boldsymbol{u} - \mathbf{div}\boldsymbol{\sigma}_{xy} + g\boldsymbol{\nabla}_{xy}\eta = -\boldsymbol{\nabla}_{xy}\left(\frac{p_s}{\rho}\right),\\
&\frac{\partial \eta}{\partial t} + \mathrm{div}\int_{-h}^{\eta}\mathbf{u}\mathrm{d}z = 0, \qquad\qquad (12)\\
&\mathrm{div}\,\mathbf{u} + \frac{\partial w}{\partial z} = 0,
\end{aligned}$$

where the unknowns are the horizontal components of the velocity $\boldsymbol{u} = (v_x, v_y)$, the vertical component $w = v_z$ and the elevation η. Here, $\boldsymbol{\nabla}_{xy}$ is the nabla operator in the (x, y) plane, $\boldsymbol{\sigma}_{xy}$ contains the viscous contribution to the first two rows of the Cauchy stress tensor $\boldsymbol{T}$ and $p_s = p_s(x, y, t)$ is a pressure pattern acting on the free surface.

The key idea to account for the boat presence is to reformulate the problem as a constrained one. We assume that the position of the external surface of the boat at each time t can be described by a single-valued function $\Psi = \Psi(x, y, t)$, suitably extended to cover all Ω_{2D}. The constraint then reads, for all t,

$$\eta \le \Psi, \quad \text{in } \Omega_{2D}, \qquad (13)$$

where the equality applies in the region where the free surface is in contact with the body. To enforce the previous inequality we introduce a Lagrange multiplier $\lambda = \lambda(x, y, t)$. By inspection, it can be found that λ can be interpreted as a perturbation to pressure applied to the surface, that is we may write

$$p_s(x, y, t) = p_a + \lambda(x, y, t) \qquad (14)$$

where p_a is the constant atmospheric pressure (often taken equal to zero). Introducing this last expression into (12) and adding the constraint (13) to the system gives rise to a saddle point problem. It is solved by an Uzawa iterative method where the constrained problem is reduced to a sequence of unconstrained problems of the form (12).

When considering the dynamics of the scull, the value of Ψ at each time step is given by solving equations (9), where the hydrodynamic forces are computed by integrating the surface stress provided by the 3D-SW model.

From the numerical point of view, problem (12) leads to very efficient computer implementations. For the space discretisation we have adopted a finite element scheme which employs Raviart-Thomas $\mathbb{RT}_0$ triangular elements in the (x, y) plane for $\boldsymbol{u}$ and standard P^1 elements for w. The elevation η, as well as the multiplier λ, is approximated by a piecewise constant function.

It is also possible to account efficiently for non-hydrostatic effects by a change in the formulation, which we have omitted to illustrate for the sake of space. In any case, the model rely on the assumptions made on the domain shape as well as on the hypothesis that the horizontal components of water velocity are dominant w.r.t. the vertical one. This is not so limitative for rowing boats.

	$A_{\max}$	T	δ
I_{xx}	0.098L	1.21 s	0.8
$2I_{xx}$	0.080L	1.64 s	0.5

Table 1: Damped oscillation parameters for different moments of inertia

4 Results

4.1 RANS simulations

Several numerical simulations have been carried out to assess the accuracy of the model introduced in Section 2.1. The coupling between the RANS flow solver and the 6-DOF dynamical system was used to predict the ship's running attitude for a Series 60 hull in different sea conditions (see [8]).

Here we present the results concerning the stabilisation behaviour of the hull subjected to a roll forcing moment. We start from a steady symmetric solution and we impose a time dependent rolling moment given by $M_{x,\text{ext}} = 20\,H(0.5-t)(\sin(2t))^2$, where H is the Heaviside function. Under this external moment the boat reaches a maximum roll angle of about 15 degrees and then stabilises to the symmetric equilibrium state. The position of the hull and the free surface around it at different time instants during the stabilisation process are reported in Figure 2.

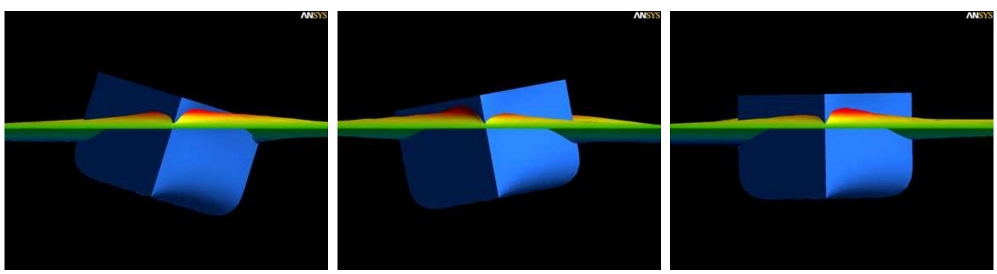

Figure 2: Bow wave around the hull at different time instants during the roll stabilisation.

The time evolution of the roll angle for two different values of the moment of inertia around the roll axis is given in Figure 3. As expected, the hull with the smaller moment of inertia reaches a larger maximal roll angle and then stabilises more quickly. In Table 1, we report the maximal amplitude of the roll angle oscillation $A_{\max}$, its period T and the damping factor defined as $\delta = \ln(\phi_j/\phi_{j+1})$ where ϕ_j is the value of the roll angle at the j-th maximum. This kind of analysis can be very useful to characterise the dynamic behaviour of a boat.

4.2 Potential model

The fluid dynamic model described in Section 3.1 has been used to compute the dynamics of a real rowing boat, a single scull, starting from the boat geometrical data, physical characteristics and kinematics of the rowers.

The output is depicted in Fig. 4, which shows the positions and velocities along X and Z directions, as well as pitch angle and angular velocity, comparing two configuration with the same scull and rowers of different weight.

As expected, the heavier rower's boat proceeds with a deeper sinkage, determining a larger wet surface and hence higher drag, which obviously reduces his speed with respect to the lighter rower. To obtain the same performance he has to change rowing style and possibly push harder. Being able to assess rapidly the performance changes due to a modification of the rower characteristics makes this model useful also for trainers and athletes.

4.3 3D-SW model

We have considered a coaxless quad scull. The first picture in Fig. 5 illustrates the wave pattern generated by the boat moving at the constant mean velocity, computed using the model given in Section 3.2. The second and third pictures illustrate that obtained at the instant of the catch and at the release, when the full dynamics of the boat is considered. We have assumed a stroke period of 1.5 seconds.

The alteration to the wave pattern caused by the secondary motions is evident. Comparison with experimental data is currently under way. So far, we have carried out only qualitative assessment comparing the wave pattern with that obtained from video recording, with good agreements.

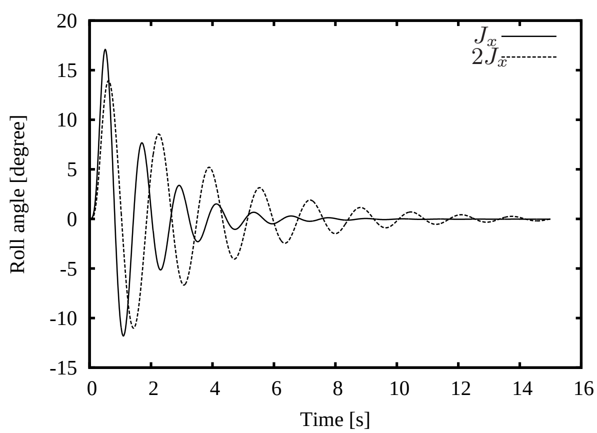

Figure 3: Time evolution of the roll angle with different moments of inertia.

5 Conclusions

We have illustrated a hierarchy of models recently developed to simulate the dynamics of boats. Each model has its own advantages and limitations. The RANS based models are in principle capable to capture the complete physics, yet they are rather costly, both in terms of the time needed to prepare of a good mesh and in terms of the computational cost of a simulation.

Reduced models are better suited in the preliminary design phase. For the case of scull dynamics we have presented two possibilities. In the simplest one the hydrodynamic forces by the mean motion are expressed by simple formula, while the effect of the secondary motions are accounted for by solving a potential problem for wave radiation. This greatly reduce the computational complexity allowing to obtain a result in a matter of minutes. Despite the simplifications made, the model is capable of giving useful indications on the boat performance. For this reason it has been implemented in a software currently used for preliminary design by a boat manufacturer.

The 3D-SW model we presented last leads to rather efficient algorithms under reasonable assumptions and has shown rather encouraging results. A full validation against experimental data is under way.

A natural further development of this study is the use of these tools for

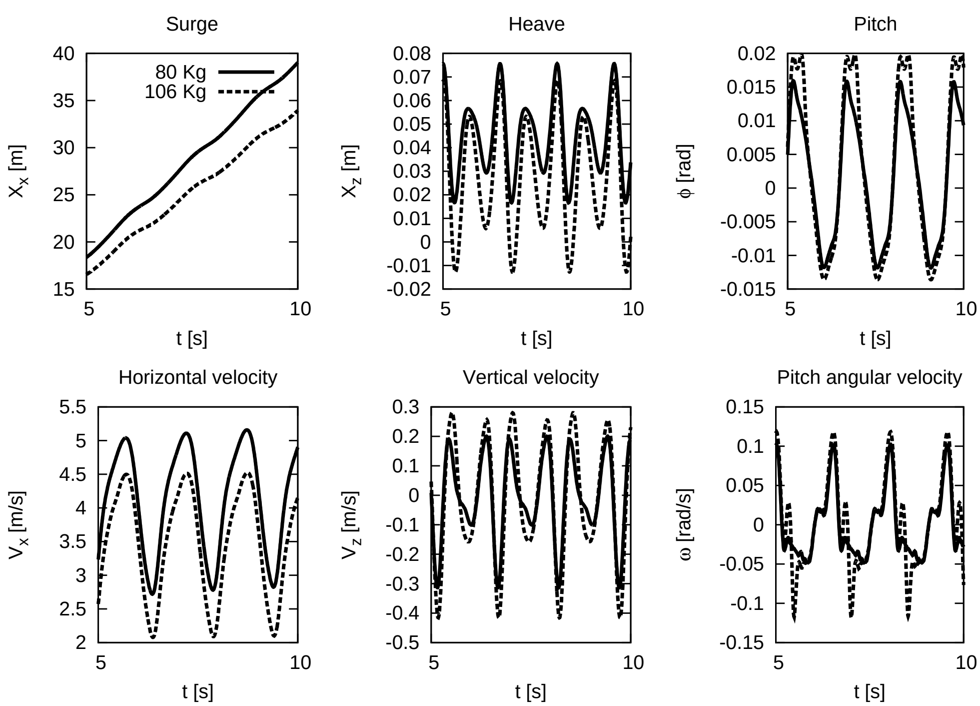

Figure 4: Positions and velocities for a single scull pushed by two different rowers. The first weighting 106 Kg (light line) and the second 80 Kg (dark line)

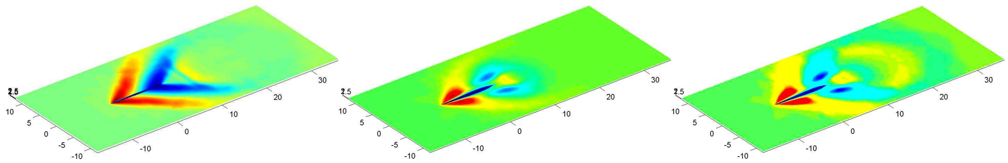

Figure 5: The surface wave pattern for the mean motion (left) and at two different time instants obtained using the full boat dynamics

automatic shape optimization.

Acknowledgements

The authors wish to thank Filippi Lido s.r.l and in particular Ing. Alessandro Placido for the financial and technical support, and for having introduced them to the world of rowing. A thank also to Matteo Lombardi and Andrea Paradiso for making available some results from their master theses.

References

[1] R. Azcueta. Computation of turbulent free-surface flows around ships and floating bodies. *Ship Technology Research*, 49(2):46–69, 2002.

[2] R. Azcueta. RANSE Simulations for Sailing Yachts Including Dynamic Sinkage & Trim and Unsteady Motions in Waves. In *High Performance Yacht Design Conference*, pages 13–20, Auckland, 2002.

[3] U. P. Bulgarelli. The application of numerical methods for the solution of some problems in free-surface hydrodynamics. *Journal of Ship Research*, 49(4):288–301, 2005.

[4] U. P. Bulgarelli, C. Lugni, and M. Landrini. Numerical modelling of free-surface flows in ship hydrodynamics. *International Journal For Numerical Methods In Fluids*, 43(5):465–481, 2003.

[5] J. Donea. Arbitrary Lagrangian Eulerian methods. In *Computational Methods for Transient Analysis*, volume 1 of *Computational Methods in Mechanics*. North-Holland, Elsevier, 1983.

[6] L. Formaggia and F. Nobile. A stability analysis for the Arbitrary Lagrangian Eulerian formulation with finite elements. *East-West Journal of Numerical Mathematics*, 7:105–131, 1999.

[7] C. W. Hirt and B. D. Nichols. Volume of Fluid (VOF) Method for the Dynamics of Free Boundaries. *J. Comp. Phys.*, 39:201–225, 1981.

[8] M. Lombardi. Simulazione numerica della dinamica di uno scafo. Master thesis (in italian), Mathematics Department, Politecnico di Milano, 2006.

[9] C.C. Mei. *The applied dynamics of ocean surface waves*. World Sceintific Publishing, Singapore, 1989. Second printing with corrections.

[10] E. Miglio, A. Quarteroni, and F. Saleri. Finite element approximation of quasi-3D shallow water equations. *Comp. Meth. Appl. Mech. Engng.*, 174(3-4):355–369, 1999.

[11] P. Mohammadi and O. Pironneau. *Analysis of the k-epsilon Model*. Masson, Paris, 1994.

[12] A. Mola, L Formaggia, and E. Miglio. Simulation of the dynamics of an olympic rowing boat. In *Proceedings of ECCOMAS CFD 2006,Egmond aan Zee, September 5-8, The Netherlands*. TU Delft, 2006. ISBN: 90-9020970-0.

[13] H. Orihara and H. Miyata. Evaluation of added resistance in regular incident waves by computational fluid dynamics motion simulation using an overlapping grid system. *Journal of Marine Science and Technology*, 8(2):47–60, 2003.

[14] N. Parolini and A. Quarteroni. Mathematical models and numerical simulations for the America's Cup. *Comp. Meth. Appl. Mech. Engng.*, 194(9-11):1001–1026, 2005.

[15] N. Parolini and A. Quarteroni. Modelling and numerical simulation for yacht design. In *Proceedings of the 26th Symposium on Naval Hydrodynamics, Rome, Italy, 17-22 September 2006*, 2007. To appear.

[16] C. Yang and R. Lohner. Calculation of ship sinkage and trim using a finite element method and unstructured grids. *International Journal of Computational Fluid Dynamics*, 16(3):217–227, 2002.